Enhancing 5G Performance: A Study of an MIMO Antenna with Elliptical Ring Polarization

P. Ramya
Department of ECE, Bannari Amman Institute of Technology, Sathyamangalam, Erode, Tamil Nadu, India
pramyabit@gmail.com (corresponding author)

G. Sunil Kumar
Department of VLSI Design & Technology, K J College of Engineering and Management Research, Pune, Maharashtra, India
gsunilmtech@gmail.com

G. Venkata Hari Prasad
Department of ECE, Anurag Engineering College, Kodad, Suryapet, Telangana, India
gvh.prasad2k@gmail.com

Berakhah F. Stanley
Department of ECE, Vel Tech Rangarajan Dr. Sagunthala R&D Institute of Science and Technology, Chennai, Tamil Nadu, India
berakhahfstanley@veltech.edu.in

C. Anna Palagan
Department of ECE, Saveetha Engineering College, Saveetha Nagar, Thandalam, Chennai, Tamil Nadu, India
annapalaganc7467@gmail.com

V. Silpa Kesav
Department of ECE, CVR College of Engineering, Hyderabad, Telangana, India
shilpakesav@gmail.com

A. Pradeep Kumar
Department of ECE, Malla Reddy Engineering College, Secunderabad, Telangana, India
pradeepkumar@mrec.ac.in

N. Rajeswaran
IMS Unison University, Dehradun, Uttarakhand, India
rajeswarann@gmail.com

Received: 6 November 2024 | Revised: 30 November 2024 | Accepted: 9 December 2024

 DOI: https://doi.org/10.48084/etasr.9516

ABSTRACT

This paper discusses the design and evaluation of a four-element Multiple-Input, Multiple-Output (MIMO) antenna array with Circular Polarization (CP), tailored explicitly for sub-6 GHz 5G wireless systems. The proposed antenna utilizes an elliptical ring slot with a variable width in the ground plane and an

asymmetric feed line layout to achieve orthogonal CP radiation in both the forward and backward directions. Three interconnected strip lines are incorporated into the ground plane for enhanced performance, increasing isolation and ensuring effective linkage between the antenna components and their respective grounds. The antenna exhibits strong isolation, a low Envelope Correlation Coefficient (ECC), and minimal Channel Capacity Loss (CCL), making it ideal for MIMO applications. The analysis confirms the antenna's stable CP gain and operational efficiency throughout the sub-6 GHz band, meeting the rigorous standards of contemporary 5G networks.

Keywords-communication; 5G; MIMO antenna; circular polarization

I. INTRODUCTION

The integration of spatial diversity has considerably improved the performance measures of wireless communication systems. The MIMO antenna technology exploits the multipath signal propagation by utilizing multiple antennas at the receiving end, enhancing channel capacity and diversity. However, methods to decouple additional elements, such as neutralizing lines, Electro-Magnetic Band Gaps (EMBGs), Frequency-Selective Surfaces (FSSs), and parasitic components, often lead to a larger antenna footprint. To tackle this issue, polarization diversity techniques are utilized to lower far-field correlation while keeping antenna sizes compact, thus decreasing the inter-element coupling and enhancing the performance metrics. In modern wireless communication systems, CP antennas are widely deployed because they effectively reduce the impact of multipath propagation and do not depend on orientation for transmitting or receiving signals. They are especially suitable for dynamic environments, like 5G networks, where maintaining signal integrity is vital. CP antennas offer numerous advantages in MIMO systems, such as increased frequency reuse, better channel capacity, and decreased vulnerability to polarization mismatches. As a result, dual-polarized antennas with MIMO functionality have been increasingly adopted in applications, such as WLAN, C-band, and geostationary systems, over the past five years [1]. This type of antenna involves the implementation of two distinct T-shaped feed lines in conjunction with a dual Coplanar Waveguide (CPW)-fed squared antenna array, which incorporates inverted L-strips within the ground plane configuration. The Axial Ratio Bandwidth (ARBW) exhibited by this antenna is considerable. A dual CP antenna array was proposed, featuring a projecting L-shaped strip alongside an inverse L-shaped strip [2]. In a compact MIMO antenna featuring polarization diversity, three wired stubs were implemented alongside an F-shaped Defective Ground Structure (DGS) to enhance the inter-element isolation.

A triple-band MIMO configuration was developed utilizing four resonant patches with tapered corners. To enhance isolation, it is essential to maintain a significant distance between the two resonators [3]. A four-port CP antenna featuring a cross-slot-loaded patchwork and truncated corners has been proposed for application within the 5.8 GHz WLAN band. The implementation of a two-arm feed system effectively stimulated the resonating components. The CP MIMO antennas were limited to generating Right-Hand Circularly Polarized (RHCP) waves and exhibited dual CP but demonstrated notably small axial ratios and limited impedance bandwidths. In [4], it was demonstrated that low-cost multimode patch antennas can support dual MIMO configurations and facilitate enhanced localization. The antenna displayed a range of operational modes while achieving notable isolation, gain, and localization accuracy. An innovative MIMO antenna design featuring compact, decoupled antenna pairs was specifically optimized for 5G mobile terminals [5]. The proposed solution effectively tackles mutual coupling challenges and enhances MIMO performance by employing advanced decoupling techniques. Authors in [6] examined strategies for minimizing the dimensions of self-isolated MIMO antenna systems specifically designed for 5G mobile devices. In [7], the antenna structure was effectively optimized, leading to a notable reduction in size while maintaining performance integrity. In [8], a novel two-port same-polarized rectangular patch antenna was introduced, explicitly designed for MIMO access-point antenna applications. The antenna demonstrates the excitation of two out-of-phase TM10 modes, achieving impedance matching S11 and S22 values below 25 dB, port isolation S12 below 15 dB, an ECC under 0.02, and an antenna efficiency exceeding 92% within the fifth-generation frequency band of 3.4–3.8 GHz [9]. Authors in [10] introduced differential filtering broadband MIMO slot line antennas, which exhibit enhanced suitability for differential signal operation owing to their direct integration with balanced circuits. The measurement and simulation results are consistent with each other [11]. In [9], a dual-polarized antenna was demonstrated, utilizing a vector synthetic process for Massive MIMO, representing a significant advancement in wireless communication research. The antenna array can generate diverse patterns to meet the specific demands of the communication network, including a high front-to-back ratio, reduced side lobes, enhanced isolation, and minimized cross polarization [12]. In [13], a thin strip MIMO antenna featuring dual polarization was applied in a 5G mobile phone technology. The proposed antenna design allows for integrating a compact, pony-sized MIMO antenna within a mobile phone, optimizing space utilization without compromising the internal volume or ground clearance [14]. An innovative, cost-effective multi-mode patch antenna exhibits robust MIMO capabilities and accurate Angle of Arrival (AoA) estimations [15]. Enhancing the localization algorithm support facilitates the development of straightforward and cost-effective MIMO solutions [16]. The construction of an array of radiating patches utilizing alternate modes has improved MIMO performance, particularly in scenarios characterized by an uncertain angle of arrival [17]. The key benefits of the proposed scenario include:

- An orthogonal CP 4-element MIMO antenna design that improves performance for 5G cellular applications.
- The use of an uneven feed line layout with an elliptical ring slot, having a non-uniform width in the ground plane to produce CP and increase antenna efficiency.

- It shows strong performance in terms of the low ECC, CP gain, and isolation, suggesting an efficient MIMO operation.

II. METHODOLOGY

A. Design of Antenna Elements

The G-shaped monopole radiator of the monopole antenna element is fabricated on a cost-effective FR-4 substrate with dimensions of L1 W1 = 25 × 25 mm² (relative permittivity, r = 4.4; loss tangent, tan = 0.02; thickness, t = 1.6 mm) and is energized by a 50 Ohm microstrip line feed. A vertical line strip incorporates the fundamental mode into two orthogonal modes. The introduction of the vertical line strip effectively increases the path length traversed by the surface current, thereby expanding the impedance bandwidth [4]. An arc is excavated in the substrate in a circular configuration to enhance impedance matching at elevated frequencies. In the initial phases, the vertical line strip of the antenna is incorporated, followed by an adjustment to the length of the C-shaped radiator. Also, a linear strip is added by incorporating a peak current length, which enhances impedance matching across the specified frequency range [8]. The evolutionary stages of the proposed CP monopole antenna are presented in Figure 1.

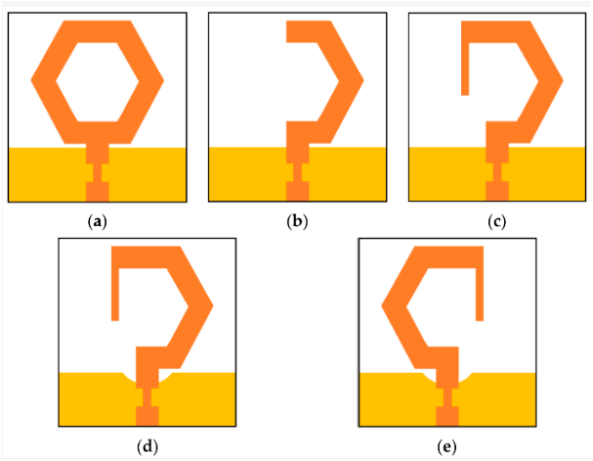

Fig. 1. CP monopole antenna stages: (a) Antenna 1, (b) Antenna 2, (c) Antenna 3, (d) Antenna 4, (e) Mirror of Antenna 4.

A reference line strip on the CP Antenna preserves the magnitude ratio (Ex/Ey) and the 90° modulation index between the azimuth and elevation electric fields, as depicted in Figure 1(c). To improve the impedance matching, an arc-shaped section of the rectangular ground plane beneath the radiator has been modified, as illustrated in Figure 1(d). CP can be generated by interacting with two orthogonal resonant frequencies with equal magnitudes and a phase difference of 90°.

B. Circularly Polarized Antennas

The CP MIMO antenna consists of two identical antenna components, Ant.1 and Ant.2. These components are fabricated on a cost-effective FR-4 substrate, the measurements of which are: 25 mm by/x 20 mm by/x 1.6 mm, and features partial grounds with W and L1 dimensions. Ant.1 serves as a mirror image of Ant.2, and their configuration may facilitate the generation of RHCP and LHCP waves, attributable to the diversity in polarization [9]. The spacing between the centers of the two antenna components, including a minor air gap, is calibrated to 0.16 to achieve sufficient isolation. The structure comprises two concentric rings, r2 and r3, alongside one circular patch, r1, and another circular patch, r3, forming each antenna element, namely Ant.1 and Ant.2, all of which share a common center position denoted as 'O'. The 3D electromagnetic simulator CST MWS R replicates the characteristics of the CP MIMO antenna, which incorporates SMA connectors. Figure 2 illustrates the design layout of the proposed CP MIMO-diversity antenna, along with its associated parameters and optimal values.

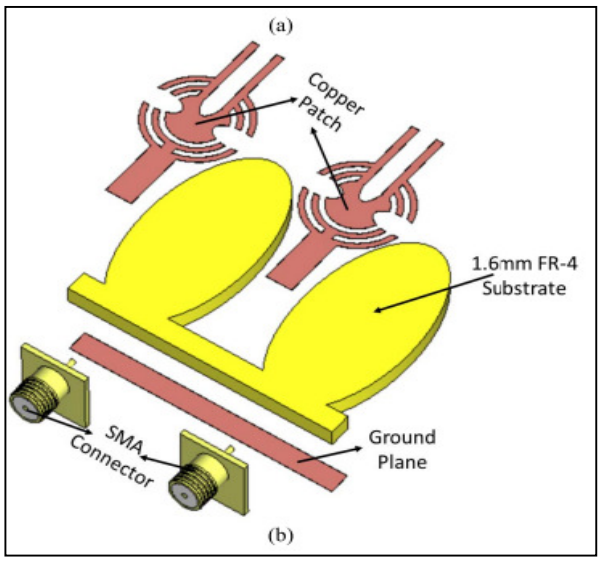

Fig. 2. Breakdown view of the proposed antenna.

Implementing the MIMO wireless technology presents significant opportunities for enhancing wireless systems' data throughput, capacity, and reliability by utilizing multiple pathways for data transmission and reception [18]. The MIMO system, currently applied in 4G user equipment, has the potential to be implemented in future 5G mobile terminals. The design of the antennas necessitates a careful consideration of various factors, including low profile, ease of manufacture, and effective isolation, among others. The current study investigates the fundamental characteristics of a single-element dual-polarized square-ring slot resonator, detailing both the modeling and experimental results obtained. Table I presents the parameter values for both the MIMO array and the single-element antenna.

The findings indicate that the positioning of the parasitic structures substantially impacts both the mutual coupling characteristics and the frequency response of the antenna. The fourth configuration presented in Figure 3 emerges as the most effective alternative, exhibiting the strongest correlation with the S11 or S22 characteristics within the specified frequency range, 3.4 to 3.8 GHz 5G band. The width of the square-ring

slot can be easily modified to tailor the antenna response, as evidenced by the simulated S11 curves corresponding to different slot-ring diameters (W). The distribution of currents has predominantly occurred around the square-ring slot radiator situated in the ground plane. This observation indicates that the currents exhibit opposing directions at the different feeding ports, leading to dual polarization characteristics. The network analyzer was employed to assess the S11 or S22 and S21 or S12 characteristics, while the anechoic chamber facilitated the investigation of the antenna radiation pattern.

TABLE I. DESIGN PARAMETER VALUES

Parameter	Value (mm)
W	13.4
hs	1.6
Wf	3
Lf	11.75
Ws	30
W1	11.9
W2	13.15
S	0.75
S1	0.75
L1	9
D	5.95
r	3

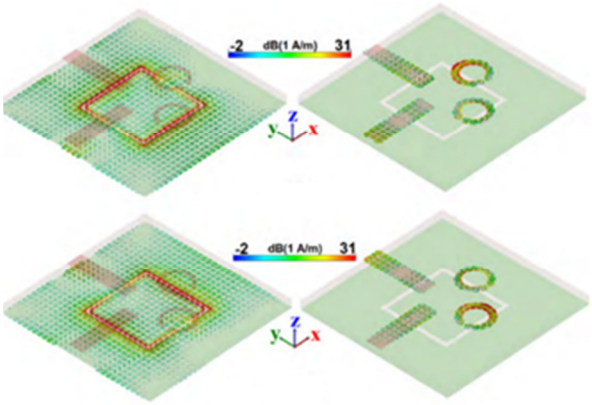

Fig. 3. Current distribution for 3.6 GHz across various ports.

C. Proposed Design of Single and MIMO Antenna

A feed line mechanism characterized by an unequal flow rate and an elliptical ring slot is employed to achieve continuous processing for each element. Each antenna element exhibits a horizontal and vertical reflection of its neighboring element. The proposed MIMO antenna has the potential to function effectively within the designated frequency spectrum for 5G wireless sensor network applications, as portrayed in Figure 4. The MIMO antenna is composed of four distinct antennas that are arranged in a configuration, where their mirror images surround them. It can potentially emit LHCP and RHCP waves in opposing directions.

Implementing MIMO antennas presents a significant opportunity to realize MIMO diversity across the spectrum. Each antenna element exhibits a significant 10 dB impedance and a 3 dB AR bandwidth encompassing the required frequency range. Based on the obtained results, the performance of the MIPO antenna is enhanced in the relevant frequency bands. Furthermore, the effects of the user's hand on the MIMO antenna are analyzed, yielding significant findings. The CP MIMO antenna system design is focused on its application in the Radio Frequency Identification (RFID) technology. The antenna incorporates an air gap substrate to facilitate the attainment of a wide bandwidth. The antennas are examined to determine their resonance frequency and bandwidth.

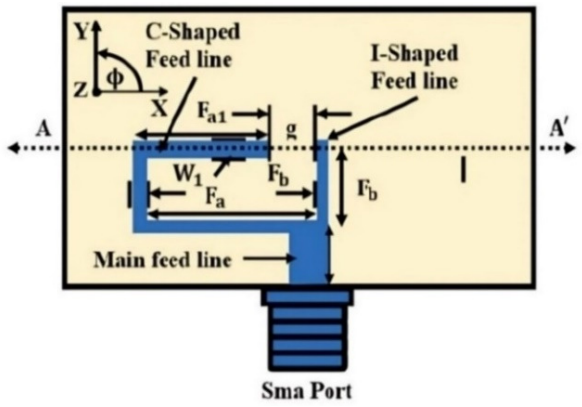

Fig. 4. MIMO antenna with feed lines.

An extensive evaluation of the antenna's bandwidth features was performed, focusing primarily on the return loss, S11, and impedance alignment. Throughout the sub-6 GHz spectrum, the antenna maintains an S11 value lower than -10 dB, confirming efficient impedance matching. The results verify the antenna's dependable 5G communication capability within the specified frequency band.

III. RESULTS AND DISCUSSION

A. Design

The antennas under consideration have been meticulously designed and simulated using the Ansys Electronics Desktop (AED) student software version 21. The AED is a robust platform that facilitates the design and simulation of electrical, electronic, and electromagnetic (EM) components, devices, and systems for electrical engineers. This platform serves as a cohesive interface for creating and analyzing EM, thermal, and circuit designs. The integrated strip lines are pivotal in enhancing the performance of the proposed MIMO antenna by effectively lowering mutual coupling and ensuring suitable impedance matching across the sub-6 GHz frequency range. The strip lines are designed to reduce electromagnetic interference between the antenna elements, resulting in S12 values of less than -15 dB, which is crucial for the adequately functioning high capacity 5G MIMO systems. Optimizing the existing distribution within the antenna structure enables efficient impedance matching, maintaining the return loss and S11, values below -10 dB throughout the entire frequency bandwidth. The combination of improved isolation and impedance matching underscores the vital importance of integrating strip lines to provide reliable and efficient antenna performance in modern wireless communication systems. The design achieves a gain of 3.55 dB, closely aligning with the

anticipated value. This gain is derived from a 3D gain plot, which is consistent with the design specifications. The gain is intricately linked to directivity. However, it serves as a comprehensive measure that incorporates both the efficiency of the antenna and its directional characteristics. The absolute gain of an antenna is characterized as the ratio of the intensity in a specified direction to the radiation intensity that would result if the power received by the antenna was radiated isotropically. The quantity of energy emitted by the antenna is referred to as its radiated volume of energy. The design demonstrates optimal characteristics regarding gain and directivity. The computed directivity value is 23.6687 dB, while the measured value is 22.909 dB, indicating proximity between the two results.

B. Radiation Pattern

The radiation pattern concept in antenna design pertains to the directional characteristics of the radio wave strength emitted from the antenna or similar sources. An antenna's radiation pattern and gain characterize its symmetry in the emission or absorption of electromagnetic radiation, contingent upon its operational mode as either a transmitter or receiver. The parameters are typically specified for the antenna's operational frequencies, as they exhibit variability with changes in frequency. When analyzing antenna elements, it is common practice to employ the far-field approximation when examining their radiation behavior.

C. S-Parameter

The S-parameters, often called S-matrix or scattering parameters, characterize the linear behavior of the RF electronic circuits and components. The S-parameter matrix is a foundational tool for deriving various characteristics of linear networks, including the gain, loss, impedance, phase group delay, and Voltage Standing Wave Ratio (VSWR). The S-parameters for this antenna are delineated across four distinct plots, namely plot 1, plot 2, plot 3, and plot 4. Figure 5 displays the S parameter plot 1, presenting the relationship between frequency (GHz) and dB. The scattering parameter characterizes the electrical behavior of linear electrical networks in response to various steady-state stimuli induced by electrical signals.

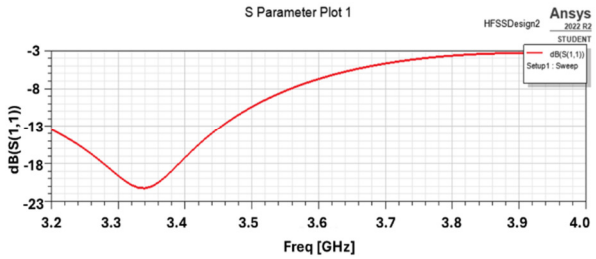

Fig. 5. Relationship between frequency (GHz) and dB.

D. Y-Parameter

The admittance parameters, commonly called Y-parameters, represent the elements of an admittance matrix, or Y-matrix. These properties find applications across various domains within electrical engineering, including power systems, electronics, and telecommunications. Figure 6 depicts the current response at port 1 obtained through simulation, using Y parameters.

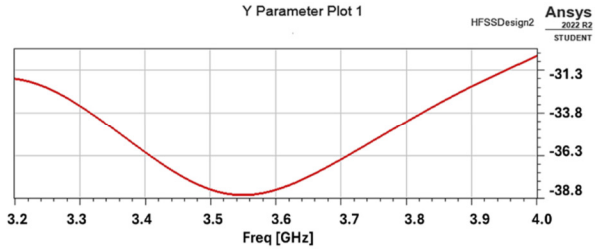

Fig. 6. Y-Parameter.

E. Z-Parameters

The impedance parameters, commonly called Z-parameters, represent the elements of an impedance matrix, or Z-matrix. These parameters are essential in electrical, electronic, and communication system engineering, as they provide a framework for characterizing the electrical behavior of the linear electrical networks. These descriptions also characterize the small-signal (linearized) response of non-linear networks. The Z parameters are frequently used with the Y, h, and ABCD parameters for modeling and analyzing transmission lines. Figure 7 illustrates the Z parameter plot, presenting the relationship between frequency and dB. The Z parameter is a critical metric for assessing an antenna's quality factor, providing valuable insights into the achievable bandwidth.

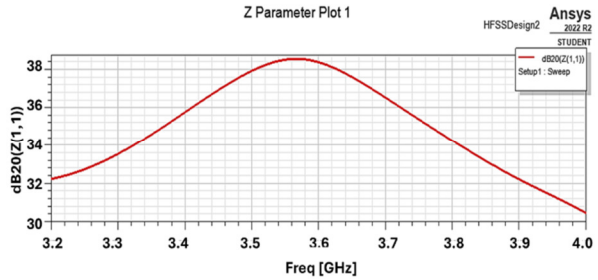

Fig. 7. Z-Parameter.

The suggested antenna demonstrates impressive performance, though, certain limitations are worth mentioning. Specifically, its effectiveness declines at the higher end of the sub-6 GHz band. Also, its manufacturing complexity is heightened due to the elliptical ring slot and connected strip lines. These limitations significantly impact its scalability and practical use in specific scenarios. The performed analysis shows the superior isolation achieved by the proposed design, as mutual coupling values consistently remain below -15 dB, outpacing many current models in the industry. Furthermore, the antenna demonstrates improved impedance matching across the sub-6 GHz range, with return loss values consistently below -10 dB. A stable axial ratio indicates improved CP performance and distinguishes the proposed solution from other options. This analysis underscores the antenna's suitability for modern 5G MIMO applications, offering a compact, high-performing solution for advanced wireless networks. The antenna

configuration consistently delivers CP across a substantial segment of the sub-6 GHz spectrum, ensuring dependable performance for diverse 5G applications. However, slight variations in the axial ratio and gain occur near the upper-frequency bounds, which might affect performance in those areas.

IV. CONCLUSION

This paper thoroughly investigates a 4-element Multiple-Input, Multiple-Output (MIMO) antenna meticulously designed for sub-6 GHz 5G wireless applications, utilizing elliptical ring slots to achieve Circular Polarization (CP). The introduced design features several groundbreaking components, including the effective use of spheroid fields with interconnected strip lines to enhance isolation and secure impedance matching. The antenna's performance has been meticulously validated via simulations and measurements, showcasing exceptional Envelope Correlation Coefficient (ECC) and Channel Capacity Loss (CCL) characteristics that meet the challenging demands of the MIMO systems. This study underscores the importance of user proximity, such as head or hand, on antenna performance, making hypotheses about its possible effects due to the primary radiation and mutual coupling interactions. The orientation of the antennas in both vertical and horizontal planes has been carefully studied to ensure reliable functionality in complex environments. The results show that the antenna operates effectively within the designated frequency range, maintaining a consistent CP gain and effective radiation patterns. Compared to similar research, the described antenna demonstrates significant advancements in isolation, improved ECC, and superior CCL performance while maintaining a compact structure, which makes it highly suitable for advanced 5G MIMO applications. This contribution confirms the viability of the proposed design and enriches the current body of knowledge by introducing novel techniques for CP generation and MIMO optimization. The results highlight the antenna's crucial role in enhancing high-capacity wireless communication systems, particularly in the developing 5G spectrum.

REFERENCES

[1] L. Pollayi and D. R. Krishna, "Design and Analysis of Wideband Cross Dipole Antenna with Bent Arms for Base Station Applications," *Progress In Electromagnetics Research C*, vol. 139, pp. 119–197, 2024.

[2] X. Teng, Y. Hou, C. Guo, S. Wang, and K. Ma, "Broadband Low-Profile Multifunction Dual-Polarized Dipole Antenna and Array for 5G and WiFi Application," *IEEE Antennas and Wireless Propagation Letters*, vol. 23, no. 6, pp. 1849–1853, Jun. 2024, https://doi.org/10.1109/LAWP.2024.3371495.

[3] X. Li, S. Wang, and W. An, "Design of tri-band dual-polarized base station antenna for 2G/3G/4G/5G," *Wireless Networks*, vol. 30, no. 3, pp. 1633–1642, Apr. 2024, https://doi.org/10.1007/s11276-023-03614-z.

[4] T. Y. Yan, X. H. Ding, J. Y. Yang, and J. X. Chen, "A Low-Cost Compact Dual-Polarized Patch Antenna Array for 5G Massive MIMO Base Station," *IEEE Antennas and Wireless Propagation Letters*, vol. 23, no. 4, pp. 1381–1385, Apr. 2024, https://doi.org/10.1109/LAWP.2024.3356531.

[5] Z. A. Shamsan, "Statistical Analysis of 5G Channel Propagation using MIMO and Massive MIMO Technologies," *Engineering, Technology & Applied Science Research*, vol. 11, no. 4, pp. 7417–7423, Aug. 2021, https://doi.org/10.48084/etasr.4264.

[6] M. Muhsin, A. Salim, and J. Ali, "A Compact Self-Isolated MIMO Antenna System for 5G Mobile Terminals," *Computer Systems Science and Engineering*, vol. 42, no. 3, pp. 919–934, 2022, https://doi.org/10.32604/csse.2022.023102.

[7] Y. F. Tsao, A. Desai, and H. T. Hsu, "Dual-Band and Dual-Polarization CPW Fed MIMO Antenna for Fifth-Generation Mobile Communications Technology at 28 and 38 GHz," *IEEE Access*, vol. 10, pp. 46853–46863, 2022, https://doi.org/10.1109/ACCESS.2022.3171248.

[8] K. L. Wong, Y. Y. Huang, and W. Y. Li, "Compact 8-Port 2×2 Array Based on Dual-Polarized Patch Antennas With Modified Cavity Field Distribution for Enhanced Port Isolation for 5G IoT Device MIMO Antennas," *IEEE Access*, vol. 12, pp. 79311–79326, 2024, https://doi.org/10.1109/ACCESS.2024.3409355.

[9] S. S. Al-Bawri, M. T. Islam, M. S. Islam, M. J. Singh, and H. Alsaif, "Massive metamaterial system-loaded MIMO antenna array for 5G base stations," *Scientific Reports*, vol. 12, no. 1, Aug. 2022, Art. no. 14311, https://doi.org/10.1038/s41598-022-18329-y.

[10] S. Dey and S. Dey, "Wideband Highly Efficient Eight Element MIMO Antenna Using Differential Fed Open End Slot for Sub-7 GHz 5G Mobile Handset Applications," *IEEE Transactions on Circuits and Systems II: Express Briefs*, vol. 71, no. 8, pp. 3760–3764, Dec. 2024, https://doi.org/10.1109/TCSII.2024.3374729.

[11] Y. Li *et al.*, "Isolation enhancement in dual-band MIMO antenna by using metamaterial and slot structures for WLAN applications," *Journal of Physics D: Applied Physics*, vol. 55, no. 32, Feb. 2022, Art. no. 325103, https://doi.org/10.1088/1361-6463/ac708d.

[12] M. A. Sofi, K. Saurav, and S. K. Koul, "Four-Port Orthogonal Circularly Polarized Dual-Band MIMO Antenna With Polarization and Spatial Diversity Using a Dual-Band Linear-to-Circular Polarization Converter," *IEEE Transactions on Antennas and Propagation*, vol. 70, no. 9, pp. 8554–8559, Sep. 2022, https://doi.org/10.1109/TAP.2022.3161493.

[13] P. Prabhu, M. Subramani, and K. Kwak, "Analysis of integrated UWB MIMO and CR antenna system using transmission line model with functional verification," *Scientific Reports*, vol. 12, no. 1, Aug. 2022, Art. no. 14128, https://doi.org/10.1038/s41598-022-17550-z.

[14] A. E. Farahat and K. F. A. Hussein, "Dual-Band (28/38 GHz) Wideband MIMO Antenna for 5G Mobile Applications," *IEEE Access*, vol. 10, pp. 32213–32223, 2022, https://doi.org/10.1109/ACCESS.2022.3160724.

[15] L. M. K. Johny, J. Mathew, and K. Gopakumar, "Improved Trans-Z-Source Active-Neutral-Point-Clamped Multilevel Inverter With Continuous Input Current for Induction Motor Drives," *IEEE Transactions on Industrial Electronics*, pp. 1–11, 2024, https://doi.org/10.1109/TIE.2024.3419255.

[16] M. M. Hasan *et al.*, "Gain and isolation enhancement of a wideband MIMO antenna using metasurface for 5G sub-6 GHz communication systems," *Scientific Reports*, vol. 12, no. 1, Jun. 2022, Art. no. 9433, https://doi.org/10.1038/s41598-022-13522-5.

[17] S. K. Mahto, A. K. Singh, R. Sinha, M. Alibakhshikenari, S. Khan, and G. Pau, "High Isolated Four Element MIMO Antenna for ISM/LTE/5G (Sub-6GHz) Applications," *IEEE Access*, vol. 11, pp. 82946–82959, 2023, https://doi.org/10.1109/ACCESS.2023.3301185.

[18] M. Pons, E. Valenzuela, B. Rodríguez, J. A. Nolazco-Flores, and C. Del-Valle-Soto, "Utilization of 5G Technologies in IoT Applications: Current Limitations by Interference and Network Optimization Difficulties—A Review," *Sensors*, vol. 23, no. 8, Jan. 2023, Art. no. 3876, https://doi.org/10.3390/s23083876.